VOL. 10, NO. 1, JANUARY 2015 ISSN 1819-6608
ARPN Journal of Engineering and Applied Sciences

www.arpnjournals.com

EFFECT OF HIGH CO_2 CONTENT ON SCALE AND CORROSION FORMATION IN OIL PRODUCTION SYSTEMS IN A COLOMBIAN FIELD

Carmen Pinzón[1], Jairo Antonio Sepúlveda[1], José Miguel Galindo[2], Carolina Charry[2] and Jorge Iván Chavarro[1]
[1]Universidad Surcolombiana/CENIGAA, Avenida Pastrana, Neiva, Huila, Colombia
[2]Ecopetrol, Gerencia de Operaciones de Desarrollo y Producción Putumayo
E-Mail: fescobar@usco.edu.co

ABSTRACT

This work is focused on studying the effect of high-CO_2-content oil reservoirs content on scale and corrosion formation by analyzing the physical and chemical variables involved and the thermodynamical models that allow studying the mentioned phenomena. A computer software tool based on the Oddo and Thomson model was developed to predict the required conditions for the occurrence of inorganic deposition. The model uses the ionic interactions theory proposed by Pitzer which allows evaluating the effect of pressure, temperature and ion concentration presented in production/injection waters. Both literature and results from this study coincide that CO_2 effect on scale formation influences carbonate generation; however, the designed tool allows predicting most commonly scale formation types such as calcite, anhydrite, semi-hydrated gypsum, gypsum, barite, gypsum, strontium sulfate, siderite, halite at different temperature and pressure conditions. The software also allows calculating saturation indexes (IS), change of saturation index (ΔIS) and the amount of deposited mass in hydrocarbon production systems. CO_2 effect on corrosion was evaluated developing software based on the model proposed by de Waard and Lotz to calculate the corrosion velocity at a given point and to evaluate the corrosion degree. Besides, it also performs a corrosion profile to determine the most critical corrosion zones along the pipe. The formation of scale from calcite and siderite shows abundance of carbonate ions and the presence of corrosion which is normally severe.

Keywords: high CO_2 content, scale, corrosion, corrosive water.

1. INTRODUCTION

Water contains dissolved ions that contribute to the formation of electrolytic dissolutions which behavior is affected by changes in the system's thermodynamic conditions as referred by Yeboah *et al.* 1993; once the brine's solubility is exceeded precipitation takes place leading to scale deposition. Table-1 provides both the most common scale types and the variables affecting solubility in oil fields.

Tendency of carbonate deposition increases in reservoirs with high CO_2 content if the brine's physical chemistry conditions have a high precipitation potential for this type of minerals. CO_2 is water soluble and forms carbonic acid according to the chemical reaction given by Equation (1). Ion CO_3^{-2} reacts with calcium presented in formation or injection water and precipitates as calcium carbonate, Equation (2). Calcium carbonate is one of the most common scale type found in hydrocarbon systems.

$$CO_2 + H_2O \rightarrow H^+ + HCO_3^- \rightarrow 2H^+ + CO_3^{-2} \quad (1)$$

$$Ca^{2+} + CO_3^{-2} \rightleftarrows CaCO_3 \downarrow \quad (2)$$

CO_2 initially dissolved in brine starts being liberated and pressure and temperature drop along the production lines in both underground and surface. After releasing both brine pH and carbonic acid, ionization increase -Fu, McMahon, and Blakley (1998) - which leads to the growing of ionic compounds to form precipitates depending on the concentration of different ionic species in the brine.

As explained by Jiaojiao *et al.* (2011) CO_2 solubility is a function of temperature, pressure and salinity. CO_2 solubility and the thermodynamic relationships established among the phases in water-oil-gas systems in presence of CO_2 determine the magnitude of the effect of CO_2 liberation in carbonate precipitation. Oddo and Tomson (1994) presented a deposition predicting model based on Pitzer (1973)'s theory for modeling electrolytic solutions. Kan and Tomson (2010) introduced a study for integration of commonly found scale in hydrocarbon production. This model includes the effects of barite, anhydrite, gypsum, basanite, calcite strontium sulfate, halite and siderite; it is also taken into account the effects of brine pH, temperature, pressure, CO_2 and H_2S presence, system salinity, alkalinity and the presence of organic acids. The calculation of the saturation indexes of each one of the above-named minerals is performed based on the solubility constant product, osmotic coefficient and activity coefficients of each ionic compound of the brine. The activity coefficients are generated by Pitzer's theory taking into account ions' binary and ternary interactions for the calculation of virial coefficients as function of temperature, pressure, ionic strength and composition.

Table-1. Common scale forms in oil fields, after Moghadasi *et al*. (2003).

Compound	Main variables
$CaCO_3$	CO_2 partial pressure pH Temperature Pressure Total dissolved solids (TDS)
$CaSO_4 + 2H_2O$ $CaSO_4 + 1/2H_2O$ $CaSO_4$	Temperature Pressure Total dissolved solids
$BaSO_4$	
$SrSO_4$	
$FeCO_3$ FeS $Fe(OH)_2$ $Fe(OH)_3$ Fe_2O_3	Dissolved gases Corrosion Temperature Pressure pH

The first predictive models for permeability reduction by scale formation were experimental. They were mainly based upon formation damaged caused by fines, Gruesbeck and Collins (1982), Wojtanowicz, Krilov and Langlinais (1987), Rochon *et al.* (1996); these models were only applied to field data. For this, water was sampled and the results were replicated to other fields by reproducing the experiments. Later, researches focused on developing general models without using laboratory procedures were undertaken. These models are based upon the relationship of porosity reduction and its effect on permeability, Civan (2001).

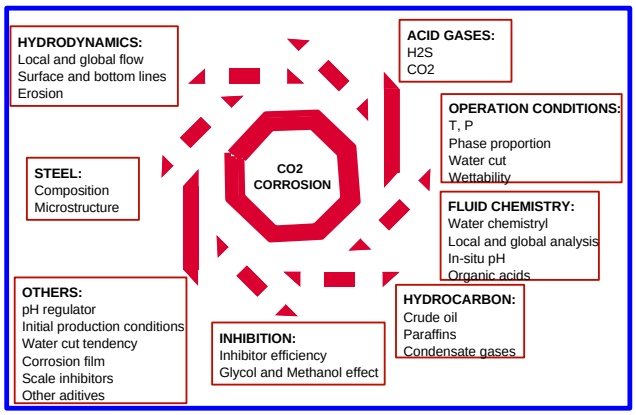

Figure-1. Factors affecting CO_2 corrosion. After Kermani and Morshed (2003).

Currently, modeling is developed from material balance in a reservoir region (commonly the near-wellbore zone) and they are related with thermodynamical models which allow quantifying the precipitated mass change as a function of reservoir pressure drop, Moghadasi *et al.* (2006), Safari *et al.* (2006), Fadairo *et al.* (2009), and Safari and Jamialahmadi (2014).

Fadairo, Omole and Falode (2009) presented a modified model for predicting permeability damage produced by inorganic deposition in oil fields at different reservoir conditions. The model includes the solid concentration change effect with pressure and the effect of porosity damage on permeability according to the following equation:

$$\frac{k_s}{k_o} = (1 - \lambda_\phi S_s (1 - S_{wi}))^3 \quad (3)$$

For the development of the reservoir model the following considerations were taken into account: (i) The precipitated solids are uniformly suspended in an incompressible fluid, (ii) isotropic and homogeneous porous medium, (iii) the rock contains a high number of pore space which are interconnected through the pore throat which obey a normal log distribution, (iv) there are no interaction forces between the medium and precipitated solid minerals.

Some authors as Kermani and Harr (1996) classify CO_2 corrosion as the most important and with highest impact among the different corrosion types presented in oil wells. Focused and general corrosion is influenced by such several factors as medium parameters, surrounding parameters, interface parameters, material or metallurgical parameters as shown in Figure-1.

de Waard and Millians (1975) published the first semi-empirical model for corrosion velocity. It was based on an electrochemical model and took only into account temperature effect and CO_2 partial pressure. de Waard and Lotz (1993) presented a quantitative model that includes several physical and chemical variables affecting corrosion velocity. This includes correction factors normally smaller than the unity that reduce corrosion velocity; otherwise, actual values would be overestimated. Among the factors we can name: iron ion concentration, pH, total pressure and protective film formation effects. Oddo and Thomson (1999) used and improved de model of de Waard and Lotz.

2. EVALUATION METHODOLOGY

Although a total of 12 wells located in the Putumayo area (Colombia) were used in this study, only corrosion and scale results for Well A are reported.

2.1. CO_2 impact on scale formation

2.1.1. Procedure for predicting scale formation

a) The first step was to collect information related to produced/injected water physical chemistry analysis and historical production data and pressure and temperature conditions required to evaluate the salt precipitation tendency. The physical chemistry analysis must content the following information:

- Brine electrolytic composition (mg/L): Barium, Calcium, Strontium, Iron, Magnesium, Manganese, Potassium, Sodium, Zinc, Bicarbonate, Carbonate, Chloride, Fluoride, Hydroxide, Sulfate, Sulfide, pH (standard conditions)
- Alkalinity (mg/L)
- Acetate (mg/L)
- TDS (mg/L)
- CO_2 composition and dissolved sulfuric acid (%)
- Production rates (Gas, oil, water)
- Pressure and temperature ranges at which is desired to evaluate the scale phenomenon

b) The above information was then introduced into a computer application developed for this study. It generates results of the scale tendency of some commonly precipitated salts. Figure-2 presents a flow chart for brine according to Oddo and Tomson model.

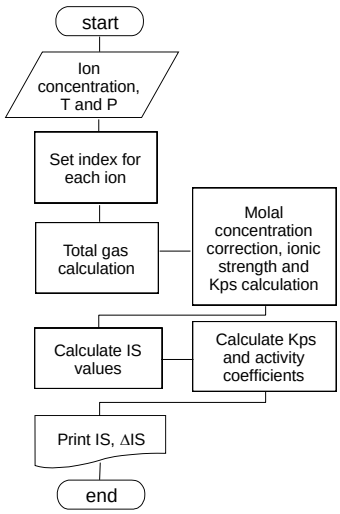

Figure-2. Flow chart based on Oddo and Tomson model for scale formation prediction.

c) After introducing the input data and the results were generated, differences among the studied zones with respect to tendencies of different scales from electrolytic brine composition were analyzed.

d) The developed computer application generates plots representing the amount of formed scale at different pressures and temperatures depending on the input ranges defined by the user.

2.1.2. Procedure for predicting scale formation in the studied area (Putumayo)

a) The information from the database provided by the Putumayo District for some wells was not enough for an accurate generation of results. Then, the additional outlined procedure was conducted:

Table-2. Physical chemical analysis of water from Well A, Average for year 2010.

Parameter	Value
Water flow rate (STBD)	40
Oil flow rate (STBD)	815
Gas flow rate (MSCF)	965
pH	7.49
Barium (mg/L)	5
Calcium (mg/L)	800
Strontium (mg/L)	5
Iron (mg/L)	25
Magnesium (mg/L)	30
Potassium (mg/L)	30
Sodium (mg/L)	800
Bicarbonate (mg/L)	400
Chloride (mg/L)	900
Sulfate (mg/L)	20
Alkalinity (mg/L)	1300
TDS (mg/L)	1000
CO_2 (%)	1.856

- Total hardness must be calculated based on the information of Calcium and Magnesium concentration with the free software available in the Water Canary Center website (FCCA).
- In some studied wells, there is no information related to the total dissolved solids (TDS) in the brine; free software available in the website of LENNTECH which uses the concentration of the different ions and anions to obtain approximated values of TDS was used for the estimation.
- Once TDS was calculated, it followed the conversion to express in terms of conductivity. It facilitated the estimation of sodium concentration.
- Since the developed software must contain non-zero information for some ions as sodium and chloride, then, calculation of sodium concentration was achieved based on pH, conductivity and total hardness previously estimated. This procedure was performed with software developed by TOSCHEM de Colombia Ltda.
- The missing alkalinity values were calculated using with the free software available in the Water Canary Center website (FCCA).

b) The input data for Well A was obtained, Table-2, after collecting and organizing the information.

c) The radial plot presented in Figure-3 was constructed based upon the data of physical chemical analysis reported during one year.

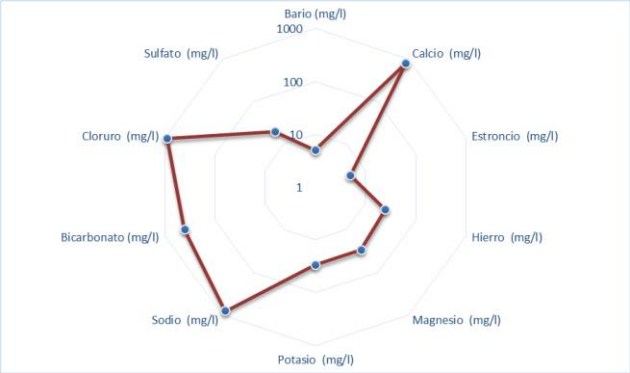

Figure-3. Average ion concentration for Well A during 2010.

Table-3 contains the results of saturation index and amount of formed precipitated for Well A at a temperature of 200 °F and pressure variation from 5000 to 50 psi. The analysis was performed for a wide range of temperature (240 °F to 80° F) and pressure (5000 psi to 50 psi) conditions. Deposition takes place when the saturation index is positive.

According to the obtained results, it can be concluded that calcite, barite and siderite have a high deposition potential at evaluated pressure and temperature conditions. On the other side, there is no deposition potential for halite, gypsum, basanite and anhydrite. It is observed for calcite and siderite that as pressure reduces, then both saturation index and amount of precipitate increase. Also, for calcite and siderite, as temperature decreases solubility decreases. If pressure decreases, the equilibrium shifts towards calcium carbonate deposition and iron (II). The barite formation case is given due to barite solubility corresponds to a very small value which with a scarce ion concentration can cause precipitation.

2.2. DEPOSITION PREDICTION RESULTS

Table-3. Results of saturation index and precipitate formation for well A based on the average of the physical chemical analysis of water for year 2010 at a temperature of 200°F and pressure ranging from 50 to 5000 psi.

		Calcite		Barite		Halite	Gypsum	Basinite	Anhidrite	Strontium sulfate	Siderite	
Pressure, psi	**pH**	**Saturation index**	**Precipitate** (lb/day)	**Saturation index**	**Precipitate** (lb/day)	**Saturation index**	**Precipitate** (lb/day)	**Saturation index**	**Precipitate** (lb/day)	**Saturation index**	**Saturation index**	**Precipitate** (lb/day)
5000	6.33	1.141292	9.2015	0.10611	0.0226	-4.9125	-1.69788	-2.0081	-1.4099	-2.409	1.77139	0.7148
4000	6.38	1.264391	9.7626	0.14294	0.0295	-4.9016	-1.66301	-1.9621	-1.36387	-2.3637	1.894489	0.7182
2000	6.62	1.618053	10.9222	0.20406	0.04	-4.8836	-1.60517	-1.8856	-1.28743	-2.2881	2.248151	0.7239
1000	6.86	1.891174	11.4492	0.22435	0.0433	-4.8776	-1.58597	-1.8602	-1.26203	-2.2635	2.521272	0.726
500	7.78	2.827923	11.7231	0.24258	0.0461	-4.8722	-1.56873	-1.8374	-1.2392	-2.2411	3.45802	0.7281
50	8.26	3.282759	12.027	0.244	0.0463	-4.8718	-1.56739	-1.8356	-1.23743	-2.2394	3.912857	0.282

3. PHYSICAL MODEL FOR FORMATION DAMAGE BY INORGANIC PRECIPITATION

The model input data were obtained from the inorganic prediction thermodynamic model based on information of physical chemistry analysis of produced water and production data.

The thermodynamic scale predictive model was run at different production periods which were organized by production changes. Six production periods resulted from 404 operation days of Well A. Uniformity of water production was the selection key as distributed and Table-4 and schematically shown in Figure-4. Precipitation tendency and amount were generated for each production interval for, later, modeling the behavior at reservoir level. The evaluation pressure interval for each period was obtained from Figure-5.

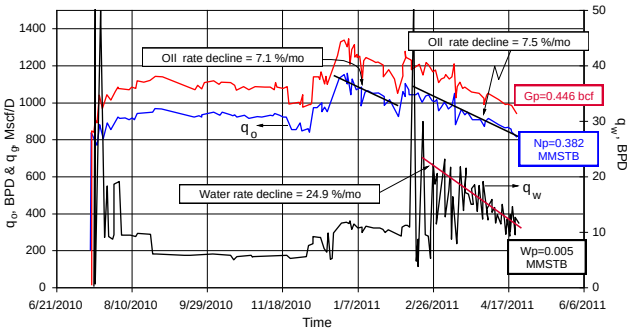

Figure-4. Production history for Well A, After Franco, C.A. *et al.* (2012).

3.1. Thermodynamic modeling results

Amount of calcite, barite and siderite deposited were generated for each time period; a sample of these results is reported in Tables 5 through 7.

Table-4. Fluid production divided by periods.

Period	*t*, days	q_w, BPD	q_o, BPD	g_g, MSCF/D
1	13	40	815	975
2	13	14	900	1050
3	26	9	925	1075
4	150	6	905	1100
5	100	8.6	970	1150
6	100	22	925	1075

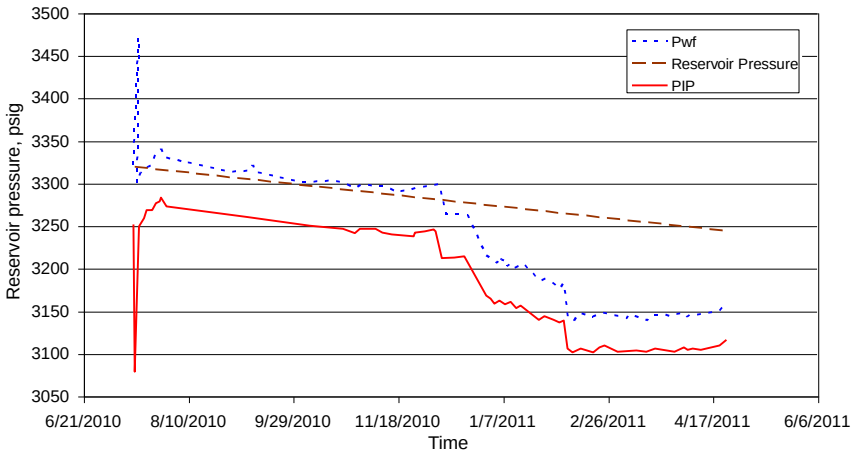

Figure-5. Pressure behavior for Well A, After Franco, C.A. *et al.* (2012).

Some input data for the reservoir physical model were obtained from using the results from the thermodynamic model for the three minerals with precipitation tendency, as outlined below:

- Water flow rate, m^3/s. A new flow rate value must be reported for each period. This is used to estimate other required parameters.
- $[dC/\rho dP]_T$. Saturation change with respect to pressure variation. This parameter is calculated for each mineral at each production period. The parameter is calculated by using the following,

$$\left[\frac{dC}{\rho dP}\right]_T = \frac{C(I) - C(F)}{\bar{P} - P_{wf}} \quad (4)$$

Table-5. Results for calcite thermodynamic modeling.

Pressure Interval for Period 1				
Pressure, psi	**pH**	**Saturation index**	**Precipitate, lb/day**	**Precipitate, mg/L**
3320 ($\bar{P}$)	7.39	2.301905	11.4552	816.99817
3300 (P_{wf})	7.39	2.304145	11.4564	817.0838
Average precipitate			11.4558	817.041

Table-6. Results for barite thermodynamic modeling.

Pressure Interval for Period 1	**Saturation index**	**Precipitate, lb/day**
3320 ($\bar{P}$)	0.0836	0.0182
3300 (P_{wf})	0.084408	0.0183

Table-7. Results for siderite thermodynamic modeling.

Pressure interval for Period-1	**Saturation index**	**Precipitate, lb/day**
3320 ($\bar{P}$)	2.930648	0.7274
3300 (P_{wf})	2.932889	0.7275

- Deposited mass (M_{dep}), g/day. It is obtained from converting the results given in lb/day to gr/day, based upon the average precipitated produced by the model according to the following thermodynamic relationship.

$$M_{dep} = Average\ precipitate\left(\frac{\text{lb}}{\text{day}}\right) * 453.59 \quad (5)$$

As for the saturation change, the deposited mass is estimated for each mineral at a given production period. Average scale concentration (C), g/m^3, for each pressure and temperature condition is the result of the average precipitation given in mg/L generated by the thermodynamic model.

The input data obtained from the thermodynamic modeling for the reservoir model are reported in Table-8. Other input data required to evaluate the effect at reservoir level are: Mineral density, (g/m^3), brine density (g/cm^3), water volume factor (bbl/STB), water viscosity (cp), formation thickness (ft), porosity, initial formation permeability (md) and wellbore radius (ft). Table-9 summarizes some input data for well A.

3.2. Procedure for the reservoir model

The computational procedure for the reservoir model is outlined below as:

a) The cumulative produced water calculation (W_p) with production data of Table-4.
b) Calculation of damage radius, (r_s). This parameter is calculated for each deposited mineral, using the below expression:

$$r_s = \sqrt{\frac{1.78731\times10^{-6}\left(\frac{\rho_w}{\rho_s}\right) * W_p * C}{\phi h} + r_w^2} \quad (6)$$

Table-8. Summary of some input data for the reservoir physical model.

Input data	Period-1	Period-2	Period-3
q_w, m^3/s	7.36065x10^{-5}	2.57623x10^{-5}	1.65615x10^{-5}
dc/dp Calcite	6.21x10^{-7}	7.39x10^{-7}	4.90x10^{-6}
dc/dp Siderite	5.17x10^{-8}	1.47775x10^{-7}	1.53248x10^{-7}
dc/dp Barite	5.17x10^{-8}	1.47775x10^{-7}	1.53248x10^{-7}
M_{dep}, gr/d Calcite	5196.24	1819.55	1169.76
M_{dep}, gr/d Siderite	329.96	115.51	74.28
M_{dep}, gr/d Barite	8.28	2.93	1.88
$C_{calcite}$, gr/m^3	817.04096	817.4322	817.4673
$C_{siderite}$, gr/m^3	51.88258	51.89124	51.90596
C_{barite}, gr/m^3	1.3016112	1.31435	1.3154792
Input data	Period 4	Period 5	Period 6
q_w, m^3/s	1.1041x10^{-5}	1.58254x10^{-5}	4.04836x10^{-5}
dc/dp Calcite	1.66x10^{-6}	3.13x10^{-6}	1.25x10^{-6}
dc/dp Siderite	2.75847x10^{-7}	6.0141x10^{-8}	2.08975x10^{-8}
dc/dp Barite	2.75847x10^{-7}	6.0141x10^{-8}	8.359x10^{-8}
M_{dep}, gr/d Calcite	779.68	1119.87	2865.42
M_{dep}, gr/d Siderite	49.51	70.96	181.50
M_{dep}, gr/d Barite	1.25	1.84	4.76
$C_{calcite}$, gr/m^3	817.29297	818.999	819.1819
$C_{siderite}$, gr/m^3	51.898	51.898585	51.8894
C_{barite}, gr/m^3	1.307555	1.343492	1.361586

Table-9. Input data for the reservoir physical model.

Parameter	Value
B_w (bbl/STB)	1.049
μ_w (cp)	0.292
h (ft)	129
ϕ (%)	10
k_o (md)	64.318
S_{wi}	0.32
r_w (ft)	0.25
ρ_{brine} (g/cm^3)	1.01
$\rho_{calcite}$ (g/cm^3)	2.71
$\rho_{siderite}$ (g/cm^3)	3.96
ρ_{barite} (g/cm^3)	4.5

c) Calculation of the deposition constant – K_{dep} (m^3/gr-s):

$$K_{dep} = \frac{q_w}{M_{dep} * t} \tag{7}$$

It is calculated for each production interval since new precipitation rates with water production changes are generated.

d) Estimate the pore volume fraction occupied by inorganic scale, *S*, using the following equation:

$$S = \frac{q^2 \left[\frac{dC}{dP}\right]_T B_w \mu_w \lambda_k}{16\pi^2 r_s^2 h^2 k_o \phi_o \rho \lambda_\phi (1 - S_{wi})(K_{dep} C)} \tag{8}$$

The above equation expresses the accumulate scale effect at different brine compositions, and such different reservoir conditions as: mineral saturation around the wellbore, brine volumetric factor, inorganic scale density, pressure drop, reservoir temperature, formation thickness, initial water saturation and radial distance from the well perforated zone.

Both permeability and porosity damage coefficients are estimated by Equations 9 and 10, respectively:

$$\lambda_k = e^{(3K_{dep} c_t)} \tag{9}$$

$$\lambda_\phi = e^{(-K_{dep} c_t)} \tag{10}$$

The pore volume fraction occupied by scale is estimated for each deposited salt: calcite, barite and siderite.

5) Estimation of permeability reduction. First, use Equation 11 to estimate the damaged permeability (k_s) caused by organic deposition.

$$k_s = k_o \left[1 - \frac{4}{3} \lambda_\phi S (1 - S_{wi})\right]^n \tag{11}$$

being *n* an empirical coefficient resulting from both the simulation and field data matching. For the studied case, *n*=1.5. The effect on permeability must be estimated for each deposited mineral.

6) Calculate the skin factor (*s*). It is estimated using the below expression:

$$s = \left(\left[1 - \frac{4}{3} \lambda_\phi S s (1 - S_{wi})\right]^{-3} - 1\right) \ln \frac{r_s}{r_w} \tag{12}$$

All the parameters used in Equation 12 were already calculated.

7) Estimation of the pressure reduction, ΔP_s, by inorganic deposition. As expected, the skin factor leads to an additional pressure drop caused by the scale presence. This is estimated with Equation 13.

$$\Delta P_s = \frac{qB\mu}{2\pi k_o h} \left(\left[1 - \frac{4}{3} \lambda_\phi S_s (1 - S_{wi})\right]^{-3} - 1\right) \ln \frac{r_s}{r_w} \tag{13}$$

Both pressure reduction and skin factor are estimated for each deposited mineral. Individual effects on permeability, skin factor and pressure drop are added according to the below expressions:

$$k_{s_{total}} = k_o - \sum_{i=1}^{n} k_{s_i} \tag{14}$$

$$s_{total} = \sum_{i=1}^{n} s_i \tag{15}$$

$$\Delta P_{stotal} = \sum_{i=1}^{n} \Delta P_{s_i} \tag{16}$$

4. RESERVOIR MODEL RESULTS

The permeability reduction, skin factor and pressure drop results, only for inorganic deposition, are graphically shown in Figures 6 to 7. Figure-8 contains the inorganic precipitation effect on permeability (circle symbols). The permeability reduction is generated by rock pore plugging caused by scale from different commonly deposited minerals (calcite, barite and siderite). In the same plot, a comparison is carried out to the modified model of Fadairo and actual data taken from the study conducted by Franco *et al.* (2012) and the results from the original model proposed by Fadairo.

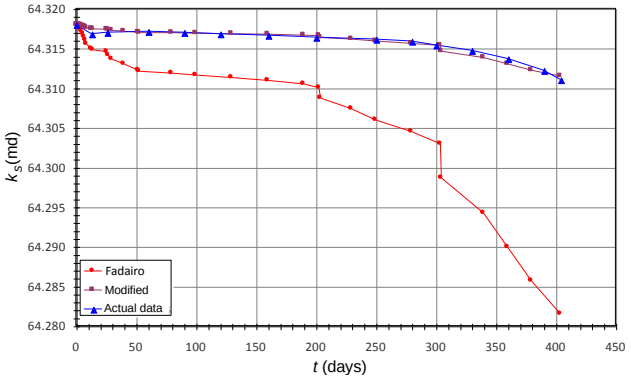

Figure-6. Reservoir model results (permeability reduction) for Well A.

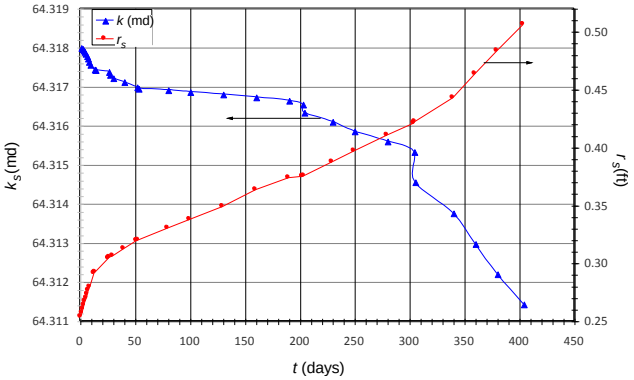

Figure-7. Inorganic deposition damage radius and its effect on permeability.

Notice also in Figure-6 the close agreement between the results obtained from the modified Fadairo model and the actual data while the original Fadairo model does not follow the actual data.

The curve matching was achieved by modifying the original Fadairo model taking into account production rate variations and the effect of salt co-precipitation.

According to the two close curves in Figure-6 (modified and actual data), the permeability damage is about 0.07 md in a time frame of 400 days. It can be then concluded that permeability damage due to inorganic deposition in minimum but it should be considered for the study of production decrease. Figures-7 and 8 report damage radius and skin factor results obtained from Fadairo model.

Figure-7 shows the increase of the zone affected by inorganic deposition; the damage radius increases approximately 100 % in 400 days of production. Figure-8 presents the skin factor and additional pressure drop as a function of time; both pressure drops and skin factor effects are very small due to the low ion concentration in the produced. This causes low precipitation levels; then, reduced effects on production.

Assuming an initial permeability value of 64.318 md and taking into account both physical rock and fluid properties; the permeability resulting from inorganic deposition is about 64.311 md in 400 days of production. In other words, 0.007 md of permeability reduction by inorganic deposition was obtained.

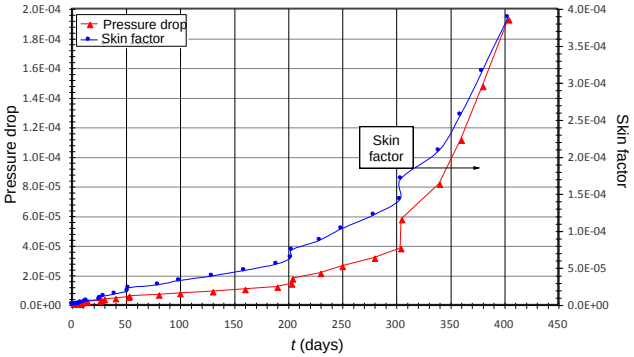

Figure-8. Skin factor and additional pressure drop due to inorganic deposition.

The calculated skin factor caused only by inorganic precipitation is 3.873×10^{-4} and the additional pressure drop caused by the same effect is of 0.31 Pa.

Using Darcy's law to estimate the average flow rate at 400 days using data from Table-9 and an initial permeability of 64.318 md, external radius of 1500 ft, formation thickness of 129 ft, external pressure of 3250 psi and well-flowing pressure of 3160 psi, the resulting monophasic ideal oil flow rate is 1105 BPD, compared to 1103.7 BPD with scale presence indicating a reduction of 1.3 BPD.

5. CO_2 IMPACT ON CORROSION

Once information was selected and organized, this was input in the developed software which is based on Waard and Lotz model. This generates the velocity corrosion in mili-inches per year, mpy.

Table-10. Predominant corrosion type. After RP0775.

Corrosion type	mm/year	mpy
Low	< 0.025	< 1.0
Moderate	0.025 – 0.12	1.0 - 4.9
High	0.13 – 0.25	5.0 - 10
Severe	> 0.25	> 10

According to Norm RP0775 of the National Association of Corrosion Engineering (N.A.C.E.), the corrosion velocity can be qualitatively classified as shown in Table-10.
The corrosion velocity results were performed for a wide range of temperature (200 to 1000 °F) and pressure (3750 psi to 2750 psi) conditions, since the system pressure and temperature were unknown. Table-11 report the corrosion velocity results for well A and the predominant corrosion type. Figures-9 and 10 show the corrosion behavior under pressure and temperature conditions, respectively, for Well A.

Table-11. Corrosion velocity for Well A.

Pressure, psi	Temperature, °F	ppCO2, psi	ppCO2 (Bar)	pH	Corrosion, mpy	Corrosion type
3750	200	30.62625	2.111605516	3.820630	9.720430	moderate
3700	195	30.2179	2.083450776	3.818520	10.824860	severe
3650	190	29.80955	2.055296035	3.816550	12.078580	severe
3600	185	29.4012	2.027141295	3.814000	13.523050	severe
3550	180	28.99285	1.998986555	3.810830	15.191650	severe
3500	175	28.5845	1.970831815	3.807710	17.457220	severe
3450	170	28.17615	1.942677074	3.804620	19.729850	severe
3400	165	27.7678	1.914522334	3.801580	22.327100	severe
3350	160	27.35945	1.886367594	3.798580	23.880760	severe
3300	155	26.9511	1.858212854	3.795620	23.196160	severe
3250	150	26.54275	1.830058114	3.792710	22.488300	severe
3200	145	26.1344	1.801903373	3.789850	21.749670	severe
3150	140	25.72605	1.773748633	3.787040	20.972590	severe
3100	135	25.3177	1.745593893	3.784280	20.149500	severe
3050	130	24.90935	1.717439153	3.781580	19.273450	severe
3000	125	24.501	1.689284413	3.778930	18.338730	severe
2950	120	24.09265	1.661129672	3.776340	17.341680	severe
2900	115	23.6843	1.632974932	3.773810	16.281500	severe
2850	110	23.27595	1.604820192	3.771350	15.161190	severe
2800	105	22.8676	1.576665452	3.768950	13.988160	severe
2750	100	22.45925	1.548510712	3.766630	12.774650	severe

CONCLUSIONS

a. High level of calcite and siderite were found for the studied Wells including Well A. Barite has lower deposition levels.
b. Inorganic deposition reduces permeability by rock pore plugging with insoluble salts that precipitate. The effect was evaluated using the modified Fadairo model which shows a production reduction due to inorganic deposition.
c. Permeability reduction resulted to be 0.003 md in 400 production days. Even though, the effect is very low, it can eventually lead to formation damage if the inorganic scale formation is not controlled.
d. The resulting corrosion velocity was severe. It demonstrates that CO_2 in presence of water forms carbonic acid which is a favorable corrosion condition.

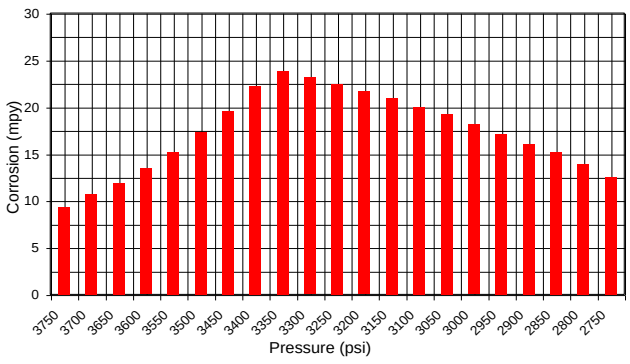

Figure-9. Corrosion vs. pressure for Well A.

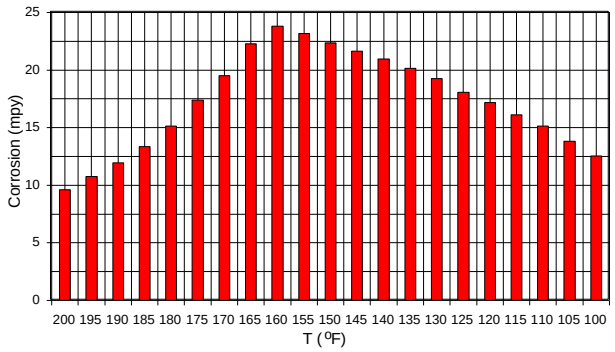

Figure-10. Corrosion vs. temperature for Well A.

ACKNOWLEDGEMENTS

The authors gratefully thank Ecopetrol, Universidad Surcolombiana and the Research Center for Sciences and GeoAgro Environmental Resources, CENIGAA, for funding this project through the mutual agreement Number 5211532.

The author also thanks Dr. Freddy Humberto Escobar, Director of agreement Number 5211532, for his cooperation in preparing this manuscript.

REFERENCES

Civan F. 2001. Modeling Well Performance under Nonequilibrium Deposition Conditions. Society of Petroleum Engineers. doi:10.2118/67234-MS. January 1.

De Waard, C. and Milliams D. E. 1975. Carbonic Acid Corrosion of Steel. Corrosion: 31(5): 177-181.

De Waard C. and Lotz U. 1993. Prediction of CO_2 Corrosion of Carbon Steel. Corrosion/1993, Paper No. 69, (Houston, TX: NACE International).

Fadairo A., Omole O. and Falode O. 2009. A Modified Model for Predicting Permeability Damage due to Oilfield Scale Deposition. Petroleum Science and Technology. 27(13): 1454-1465.

Franco C. A., Bahamon Pedroza J. I., Gonzalez Mosquera J. G., Zapata Arango J. F., Garcia C. C., Henao W. A. and Madera K. 2012. Formation Damage Modeling Improves Well Candidate Selection and Stimulation Treatment Design in Western Area of Putumayo Basin, Colombia. Society of Petroleum Engineers. doi:10.2118/152400-MS. January 1.

Fu R.K., McMahon A.J. and Blakley K. 1998. The Controversy of CO_2 Solubility in Water. Corrosion 98. pp. 92-97.

Jiaojiao G., Jienian Y., Ming C., Xiangshuang B. and Haimin S. 2011. Scale Deposition Mechanism and Low-Damage Underbalanced Drilling Fluids for High CO_2 Content Gas Reservoirs. Petroleum Exploration and Development. 38(6): 750-755.

Gruesbeck C. and Collins R. E. 1982. Entrainment and Deposition of Fine Particles in Porous Media. Society of Petroleum Engineers. doi:10.2118/8430-PA.

Kan A. T. and Tomson M. B. 2010. Scale Prediction for Oil and Gas Production. Society of Petroleum Engineers. doi:10.2118/132237-MS.

Kermani M. B. and Harrop D. 1996. The Impact of Corrosion on Oil and Gas Industry. Society of Petroleum Engineers. doi:10.2118/29784-PA.

Kermani M.B. and Morshed A. 2003. Carbon Dioxide Corrosion in Oil and Gas Production-A Compendium. Corrosion. 59(8): 659-683.

Moghadasi J., Jamialahmadi M., MülleR-Steinhagen H., Sharif A., Ghalambor A., Izadpanah M.R. and Motaie. E. 2003. Scale Formation in Iranian Oil Reservoir and Production Equipment during Water Injection. SPE 80406.

Moghadasi J., Jamialahmadi M., Müller-Steinhagen H., Sharif A., Ghalambor A., Izadpanah M. R. and Motaie E. 2003. Scale Formation in Iranian Oil Reservoir and Production Equipment during Water Injection. Society of Petroleum Engineers. doi:10.2118/80406-MS.

Oddo J. E. and Tomson M. B. 1994. Why Scale Forms in the Oilfield and Methods to Predict It. SPE Production and Facilities. pp. 47-54.

Oddo J.E. and Thomson M.B. 1999. The Prediction of Scale and CO_2 Corrosion in Oil Fields Systems. CORROSION 99, Paper No. 41, NACE.

Pitzer K.S. 1973. Thermodynamics of Electrolytes. I. Theorical Basis and General Equations. The Journal of Physical Chemistry. 77(2): 268-277.

RP0775, N. S. 2005. Preparation, Installation, Analysis and Interpretation of Corrosion Coupons in Oilfield Operations. Houston, Texas, USA.

Rochon J., Creusot M. R., Rivet P., Roque C. and Renard M. 1996. Water Quality for Water Injection Wells. Society of Petroleum Engineers. doi:10.2118/31122-MS.

Safari H. and Jamialahmadi M. 2014. Thermodynamics, Kinetics, and Hydrodynamics of Mixed Salt Precipitation in Porous Media: Model Development and Parameter Estimation. Transport Porous Media. (101): 447-505.

Wojtanowicz A. K., Krilov Z. and Langlinais J. P. 1987. Study on the Effect of Pore Blocking Mechanisms on Formation Damage. Society of Petroleum Engineers. doi:10.2118/16233-MS.

Yeboah Y. D., Samuah S. K. and Saeed M. R. 1993. Prediction of Carbonate and Sulfate Scales in Oilfields. Society of Petroleum Engineers. doi:10.2118/25586-MS.

Nomenclature

C	Concentration, g/cm^3
$C(I)$	Wellbore scale precipitation at well-flowing pressure, mg/L
$C(F)$	Scale precipitation at average reservoir pressure, mg/L
B	Volumetric factor, rb/STB
k	Permeability, md
K_{dep}	Constant depsotion rate, m^3/gs
h	Formation thickness, ft
$\bar{P}$	Average reservoir pressure, psia
P	Pressure, psi
q	Flow rate, STB/D
t	Time, hr
r	Radius, ft
r_s	Skin radius or damage radius
S_{wi}	Initial water saturation
S	Fraction of pore volume occupied by scale
s	Skin factor

Greeks

Δ	Change, drop
ϕ	Porosity, fraction
λ	Formation damage coefficient
μ	Viscosity, cp
ρ	Density, gr/cm^3

Suffices

e	External
g	Gas
i	Initial
$ideal$	Ideal
o	Oil
s	Skin
t	Total
w	Well, water
wf	Well flowing